Journal of Biomechanics 94 (2019) 99–106

Contents lists available at ScienceDirect

Journal of Biomechanics

journal homepage: www.elsevier.com/locate/jbiomech
www.JBiomech.com

Modeling methodology for defining *a priori* the hydrodynamics of a dynamic suspension bioreactor. Application to human induced pluripotent stem cell culture

Giuseppe Isu [a,b], Umberto Morbiducci [a,c], Giuseppe De Nisco [a,c], Christina Kropp [d], Anna Marsano [b], Marco A. Deriu [a,c], Robert Zweigerdt [d], Alberto Audenino [a,c], Diana Massai [a,c,*]

[a] *PolitoBIOMed Lab, Department of Mechanical and Aerospace Engineering, Politecnico di Torino, Turin, Italy*
[b] *Department of Surgery and Department of Biomedicine, University Hospital Basel, Basel, Switzerland*
[c] *Interuniversity Center for the Promotion of the 3Rs Principles in Teaching and Research, Italy*
[d] *Leibniz Research Laboratories for Biotechnology and Artificial Organ, Department of Cardiothoracic, Transplantation, and Vascular Surgery, Hannover Medical School, Hannover, Germany*

ARTICLE INFO

Article history:
Accepted 15 July 2019

Keywords:
Computational fluid dynamics
Dynamic suspension culture
Bioreactors
Working parameters
Bioprocess

ABSTRACT

Three-dimensional dynamic suspension is becoming an effective cell culture method for a wide range of bioprocesses, with an increasing number of bioreactors proposed for this purpose. The complex hydrodynamics establishing within these devices affects bioprocess outcomes and efficiency, and usually expensive *in vitro* trial-and-error experiments are needed to properly set the working parameters.

Here we propose a methodology to define *a priori* the hydrodynamic working parameters of a dynamic suspension bioreactor, selected as a test case because of the complex hydrodynamics characterizing its operating condition. A combination of computational and analytical approaches was applied to generate operational guideline graphs for defining *a priori* specific working parameters. In detail, 43 simulations were performed under pulsed flow regime to characterize advective transport within the device depending on different operative conditions, i.e., culture medium flow rate and its duty cycle, cultured particle diameter, and initial particle suspension volume. The operational guideline graphs were then used to set specific hydrodynamic working parameters for an *in vitro* proof-of-principle test, where human induced pluripotent stem cell (hiPSC) aggregates were cultured for 24 h within the bioreactor. The *in vitro* findings showed that, under the selected pulsed flow regime, sedimentation was avoided, hiPSC aggregate circularity and viability were preserved, and culture heterogeneity was reduced, thus confirming the appropriateness of the *a priori* method. This methodology has the potential to be adaptable to other dynamic suspension devices to support experimental studies by providing *in silico*-based *a priori* knowledge, useful to limit costs and to optimize culture bioprocesses.

1. Introduction

In the last decades, dynamic suspension culture has proven to be beneficial in promoting cell proliferation and in maintaining cell functionality *in vitro* (Godara et al., 2008; Rodrigues et al., 2011). Compared to conventional two-dimensional (2D) culture, three-dimensional (3D) dynamic suspension allows for the spatial 3D growth of cells/constructs, with or without the use of synthetic microcarriers (Kropp et al., 2017). Moreover, when culture encompasses proper dynamic suspension and mixing, this approach (1) minimizes the formation of gradients, (2) enhances oxygen and nutrients transport, and (3) prevents sedimentation of cultured cells/constructs (Cherry, 1993; Zweigerdt, 2009). Optimized culture conditions guarantee efficient, space- and labour-effective processes, finally resulting in more financially sustainable procedures (dos Santos et al., 2013; Kumar and Starly, 2015; Warnock and Al-Rubeai, 2006). Nowadays, dynamic suspension culture is mostly performed by stirred tank bioreactors, especially employed for scalable cell production and stem cell differentiation (Abecasis et al., 2017; Kempf et al., 2014; Olmer et al., 2012). However, several challenges remain to be addressed in case of cells highly sensitive to the surrounding chemico-physical environment, such as the human pluripotent stem cells (hPSCs). For instance, the

* Corresponding author at: Department of Mechanical and Aerospace Engineering, Politecnico di Torino, Corso Duca degli Abruzzi 24, 10129 Turin, Italy.
E-mail address: diana.massai@polito.it (D. Massai).

https://doi.org/10.1016/j.jbiomech.2019.07.021
0021-9290/

presence of the impeller in combination with the position of the analytical probes and the imposed agitation rate can induce complex hydrodynamics within stirred tank bioreactors, resulting in localized areas of turbulence and detrimental shear stresses (Rodrigues et al., 2011). Indeed, in case of hPSCs, non-physiological shear stresses can affect cell viability and growth (Leung et al., 2011; Olmer et al., 2012; Zweigerdt et al., 2011) and disrupt the sensitive equilibrium of pluripotent proliferation versus differentiation, eventually inducing undesired culture heterogeneity (Schroeder et al., 2005; Zweigerdt, 2009; Zweigerdt et al., 2011). Thus, to assure cell viability, proliferation, and/or stemness preservation, the fluid dynamics establishing within these devices should be strictly controlled (Gupta et al., 2016; Ismadi et al., 2014; Kinney et al., 2011). In recent years, experimental and computational methods have been adopted to characterize the fluid dynamics inside bioreactors, boosting the progress in bioreactor technologies, and reducing the use of trial-and-error approaches for bioprocess optimization (Guilak et al., 2014; Kaiser et al., 2012; Sucosky et al., 2004; Pennella et al., 2012; Williams et al., 2017; Wu et al., 2014; Zhao et al., 2018). The need for a comprehensive characterization of transport phenomena within bioreactors has encouraged the development of culture devices with more controllable and defined flow features (Dusting et al., 2006; Singh et al., 2005; Thouas et al., 2007). In parallel, computational approaches have become essential not only in supporting the bioreactor design, but also in optimizing the entire bioprocess, virtually monitoring physical and chemical quantities that are otherwise difficult to measure (Consolo et al., 2009; Consolo et al., 2012). In this context, a versatile bioreactor for dynamic suspension culture, characterized by the absence of rotating components and tunable ultralow-to-moderate shear stress conditions within the culture chamber, was recently proposed and applied (Massai et al., 2016; Rosellini et al., 2018). The fact that the practical use of most culture devices cannot be established *a priori*, and that diverging needs related to the specific cell/construct culture strategy could lead to an overall loss of efficiency, makes this bioreactor a paradigmatic example of the complexity in properly managing dynamic suspension devices for tissue engineering and regenerative medicine applications.

In this study we propose a methodology, based on the combination of *in silico* and analytical approaches, which uses quantitative analyses of hydrodynamics in a dynamic suspension bioreactor for defining *a priori* its hydrodynamic working parameters. The proposed methodology led to the definition of operational guideline graphs for the bioreactor use. An explanatory proof-of-principle test was carried out by culturing aggregates of human induced pluripotent stem cells (hiPSCs) within the bioreactor, whose hydrodynamic working conditions were identified through the operational guideline graphs without performing preliminary *in vitro* tests. The general nature of the proposed methodology makes it adaptable to other dynamic suspension devices for supporting experimental studies, limiting costs, and ultimately optimizing bioprocesses.

2. Materials and methods

2.1. Dynamic suspension bioreactor

An impeller-free dynamic suspension bioreactor was considered as a test case, because of the complex hydrodynamics characterizing its operating condition (Massai et al., 2016). The bioreactor is made of a culture chamber connected to a closed-loop recirculation circuit (Fig. 1A), to be located within a standard incubator (37 °C, 5% CO_2, 85–90% humidity). Briefly, the functioning of the bioreactor is based on the recirculation of the culture medium inside the culture chamber, under laminar flow regime. The presence of a check valve and of a filter confines suspended particles inside the culture chamber (Fig. 1B). The establishment of buoyant vortices within the culture chamber guarantees the dynamic suspension and mixing of cells/aggregates, in the following referred to as particles, under ultralow-to-moderate shear stress conditions (Massai et al., 2016). A non-stationary flow regime based on periodic, pulsed flow waveforms was developed in this study both to assure particle suspension and to avoid prolonged contact of the particles with the filter and possible consequent adhesion.

2.2. Pulsed functioning mode definition

A square flow rate waveform (Fig. 2A) of time duration $T = T_{on} + T_{off}$ was imposed at the inflow section of the culture chamber. More in detail: (1) T_{on} is the time duration of the phase of the working cycle when the pump pushes the medium, the check valve opens, and particles are lifted up by hydrodynamic forces within the culture chamber (Fig. 2B); (2) T_{off} is the time duration of the

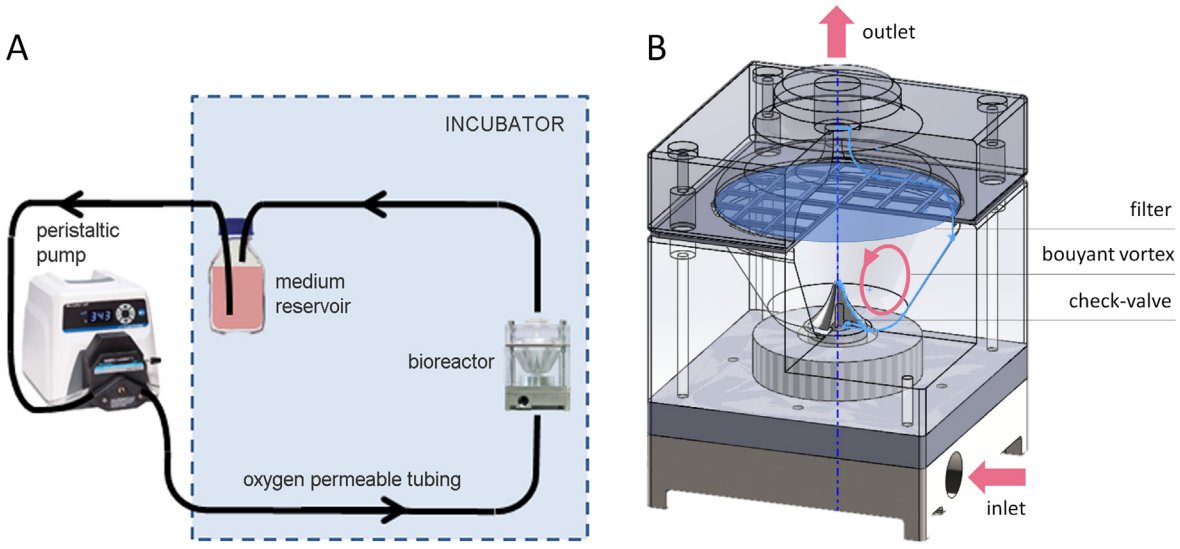

Fig. 1. Dynamic suspension bioreactor. (A) Schematic draw of the bioreactor set-up. (B) 3D model of the bioreactor culture chamber (adapted from Massai et al., 2016, license CC BY).

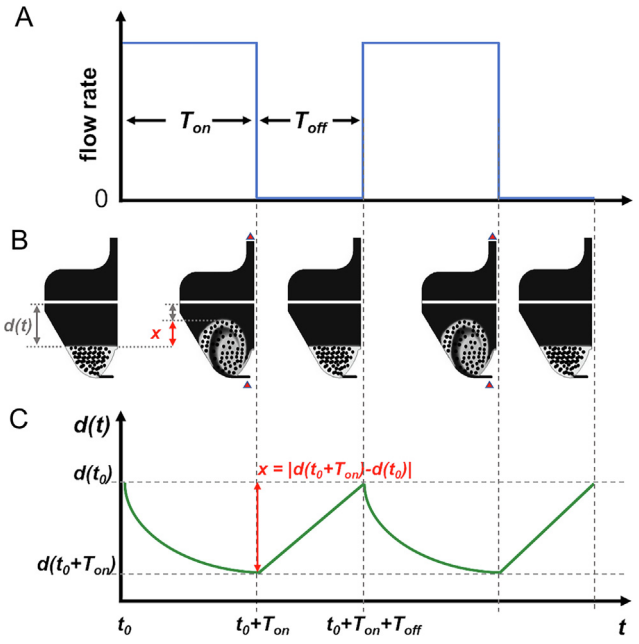

Fig. 2. Pulsed functioning mode. (A) Diagram of ideal pulsed flow rate waveform of period $T = T_{on} + T_{off}$. (B) Schematic of the particle cloud distribution within the culture chamber depending on time instant: when the pump is switched on, the check valve opens, the medium flows through the culture chamber, and particles are lifted up by hydrodynamic forces, while when the pump is switched off the flow stops, the check valve closes, and particles undergo free-fall motion due to gravity force. (C) Diagram of the distance $d(t)$ between the filter and the suspension cloud at the generic time point t: switching off the pump, the particle cloud undergoes free-fall motion and the original distance $d(t_0)$ from the filter is re-established. The variation of the distance $d(t)$ during an entire cycle is calculated as x.

phase of the working cycle when the pump is switched off and there is no net flow through the culture chamber, the check valve is closed, and particles undergo free-fall motion due to gravity force (Fig. 2B). Assuming a homogeneous distribution of particles forming a suspension cloud at time t_0, the quantity x is defined as:

$$x = d(t_0 + T_{on}) - d(t_0) \quad (1)$$

where $d(t)$ is the distance between the filter and the particle suspension cloud at the generic time point t (Fig. 2C). Technically, x represents the variation of the distance (along the vertical axis of the chamber) between the particle cloud and the filter located at the upper part of the culture chamber at the end of time interval T_{on}. When the pump is switched on at time t_0, the distance d between the suspension cloud and the filter progressively diminishes, reaching its minimum value at time $t_0 + T_{on}$. Switching off the pump, the hydrodynamic forces vanish and the gravity force causes the free-fall motion of the particles. The time duration T_{off} of the free fall motion phase can be properly set to restore the particle cloud distance from the filter up to the original value, so that $d(t_0) = d(t_0 + T_{on} + T_{off})$, contemporarily avoiding particle sedimentation at the bottom of the chamber.

Following the methodological flowchart of Fig. 3, a two-phase computational model (described below) of the hydrodynamics developing within the culture chamber was used to explore the working conditions of the device. With this approach, the distance $d(t)$ can be calculated along the time interval T_{on} starting from an initial distance $d(t_0)$, as well as quantity x, according to Eq. (1). The results of the computational simulations were then combined with the analytical calculation of the time interval T_{off}, describing the particle free-fall motion phase within the range x, using Stokes terminal velocity formulation. The combination of the computational and analytical results allowed for the quick and broad determination of the variations of $d(t)$ as a function of T_{on} and T_{off} values. Therefore, it was possible to generate operational guideline graphs useful for setting up the *in vitro* experiments.

2.3. Computational model

Here the same numerical approach proposed elsewhere (Consolo et al., 2009; Consolo et al., 2012; Massai et al., 2016)

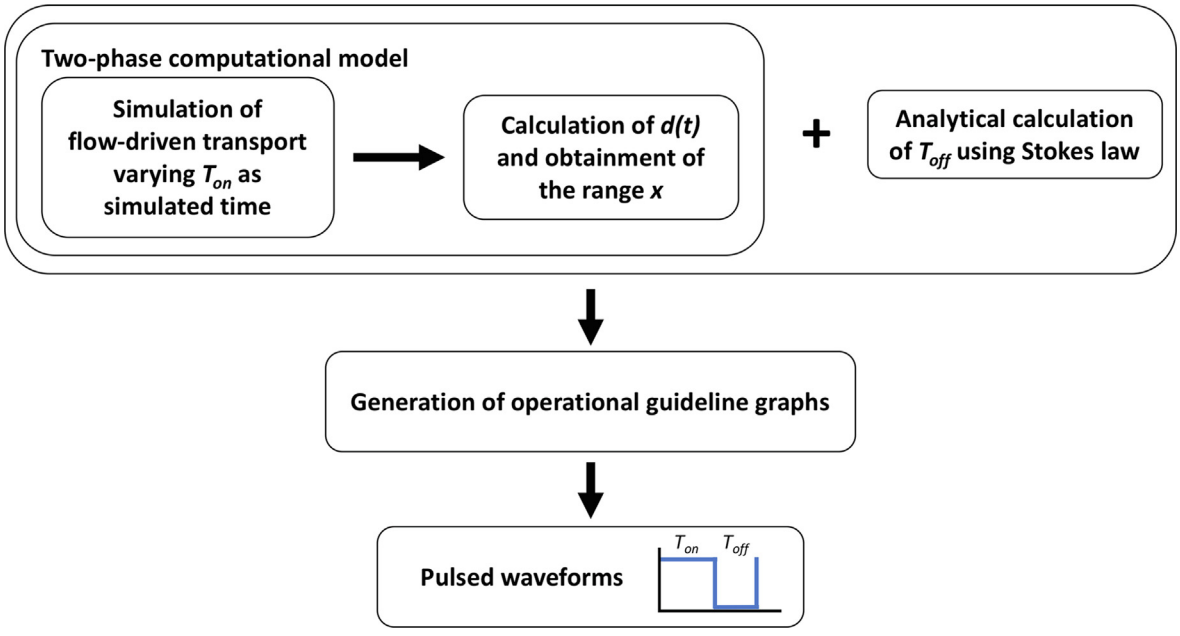

Fig. 3. Methodology workflow. Two-phase computational model of the fluid dynamics developing within the culture chamber allows exploring the working conditions of the device and calculating the distance $d(t)$ between the filter and the suspension cloud along the time interval T_{on}. The computational results are then combined with the analytical calculation of the time interval T_{off}, using Stokes terminal velocity formulation. The combination of computational and analytical results leads to the generation of operational guideline graphs useful for setting up the pulsed waveforms for *in vitro* experiments.

Table 1
Simulated conditions.

flow rate (mL/min)	particle diameter (μm)	initial particle suspension volume (mL)
30	10, 25, 50, 100	10, 25, 40
50	10, 25, 50, 100	10, 25, 40
70	10, 25, 50, 100	10, 25, 40
100	10, 25, 50, 100	10, 25, 40
100	180	10

was adopted, and a total number of 43 simulations was carried out. The final aim was to investigate the large variety of possible particle transport patterns obtainable within the bioreactor combining different conditions in terms of (1) imposed flow rate (30, 50, 70, 100 mL/min, with Reynolds numbers ranging from 12 to 35), (2) particle diameter (10, 25, 50, 100, 180 μm), and (3) initial particle suspension volume (10, 25, 40 mL), where different initial volumes imply different initial values of the distance $d(t_0)$ (Fig. S2). All simulated conditions are summarized in Table 1.

Taking advantage of the shape of the culture chamber, axial-symmetric time-dependent numerical simulations were carried out using a finite-volume commercial code (FLUENT, ANSYS Inc., PA, USA). The fluid domain was discretized with 6.5×10^3 quadrilateral cells. The Eulerian-based two-phase flow model, known as the Eulerian–Eulerian model, was implemented to simulate the concomitant, interacting presence of culture medium (primary phase) and suspended particles (secondary phase). Exhaustive details can be found in Supplementary Material. Finally, additional simulations were performed to investigate the transport of dissolved oxygen within the culture chamber (details on the computational settings are provided in Supplementary Material).

2.4. Particle free-fall motion and analytical formulation

The time interval T_{off} is governed by the free fall of suspended particles. The high dilution conditions and the low Stokes numbers here investigated, representative of realistic culture conditions, allowed the analytical calculation of free-falling particle motion when the pump is switched off. Under the simulated conditions, the free-fall terminal velocity $\vec{v}_{ff}$ of a single particle could be expressed by the dynamic balance of the Stokes drag force, the Archimedes buoyancy force, and the particle weight force, resulting in:

$$\vec{v}_{ff} = \frac{2(\rho_p - \rho_{med})R^2}{9\mu_{med}}\vec{g} \quad (2)$$

where ρ_p and ρ_{med} are particle and medium density, respectively, μ_{med} is the medium dynamic viscosity, R is the particle radius, and $\vec{g}$ is the gravitational acceleration. Applying the methodological flowchart (Fig. 3), the simulation of different time intervals T_{on} allowed obtaining a range of x values as an output, then used to estimate the corresponding range of time interval T_{off} needed to complete the working cycle as follows:

$$T_{off} = \frac{x}{v_{ff}} \quad (3)$$

This integrated approach was applied to all the combinations of flow rates, particle diameters, and initial particle suspension volumes listed in Table 1, thus generating operational guideline graphs for a broad range of possible applications.

2.5. In silico and in vitro test benching

In a perspective of future application of the applied dynamic culture device for hiPSC expansion, the combination of the computational and analytical approaches was applied to obtain operational guideline graphs useful for a hiPSC *in vitro* proof-of-concept experiment. An *in silico* experiment was performed where hiPSC aggregates were modelled as spherical particles with an average diameter of 180 μm, imposing an initial particle suspension volume of 10 mL at volume fraction (VF) equal to 2.5×10^{-2}%. Based on this setting, the operating conditions assuring dynamic suspension (imposed flow rate = 100 mL/min, T_{on} = 15 s, T_{off} = 45 s) were identified according to the operational graphs.

The effectiveness of the *in silico* approach in properly defining culture conditions was verified *in vitro*. Pre-formed hiPSC aggregates (average diameter = 180 ± 18 μm, culture protocol details in Supplementary Material) were inoculated within the bioreactor at an equivalent cell density of 0.8×10^6 cell/mL. The aggregates were kept in dynamic suspension within the bioreactor for 24 h, at the same operating conditions set for the *in silico* test (flow rate = 100 mL/min, T_{on} = 15 s, T_{off} = 45 s). As negative control, hiPSC aggregates were kept in dynamic suspension under continuous flow (flow rate = 100 mL/min). After 24 h, aggregates were harvested from the bioreactor (1) for viable-cell counting and live/dead assays (details in Supplementary Material), and (2) for assessing the preservation of their morphological features by the acquisition of light microscope images (Axio Vert.A1 microscope, Axiovision 8.4 software, Zeiss, USA). Moreover, sedimentation assessment was performed (details in Supplementary Material). Since aggregate size and the degree of aggregate homo- *vs.* hetero-geneity have been shown to substantially alter lineage differentiation and process efficiency (Zweigerdt, 2009), the aggregate circularity was quantified as a measure of aggregate fusion (fused aggregates tend to lose spherical shape), and aggregate diameters were measured in order to evaluate aggregate size distributions (ImageJ, NIH, USA). Experimental data are presented as mean ± standard deviation.

3. Results

3.1. Identification of pulsatile culture conditions

The computational approach allowed characterizing the fluid dynamics resulting from the interaction among the particle cloud, the culture chamber geometry and the pump operation. As explanatory outcome, Fig. 4 shows the contour plots of the time evolution of the particle VF imposing a T_{on} of 15 s for a simulated case (particle diameter = 180 μm, flow rate = 100 mL/min, initial particle suspension volume = 10 mL). During T_{on}, the particle cloud is gradually lifted up towards the filter by hydrodynamic forces, thus the distance $d(t)$ between the particle cloud and the filter decreases while the variation $x(t)$ of that distance increases (Fig. 4). For the sake of completeness, the results of the same simulated case extended to a time duration of 75 s are presented in Supplementary Material (Fig. S5).

For each simulated T_{on}, the calculation of distance $d(t)$ and $x(t)$, and the combination of computational results with the analytical calculations of the free-fall time interval T_{off} allowed the construction of operational guideline graphs. In particular, Fig. 5A shows the operational guideline graph for simulated particles (average diameter = 180 μm, applied flow rate = 100 mL/min, initial particle suspension volume = 10 mL). On the operational guideline graph, the initial distance $d(t_0)$ of the particle cloud from the filter is approximately equal to 18 mm (on the right y axis in Fig. 5A), and the particle cloud collides with the filter (i.e., $d = 0$) when T_{on} is equal to 16 s (on the x axis in Fig. 5A). Therefore, in order to avoid collisions of the particle cloud with the filter, a T_{on} value equal to 15 s was selected. This choice allowed guaranteeing a minimum distance between the particle cloud and the filter d

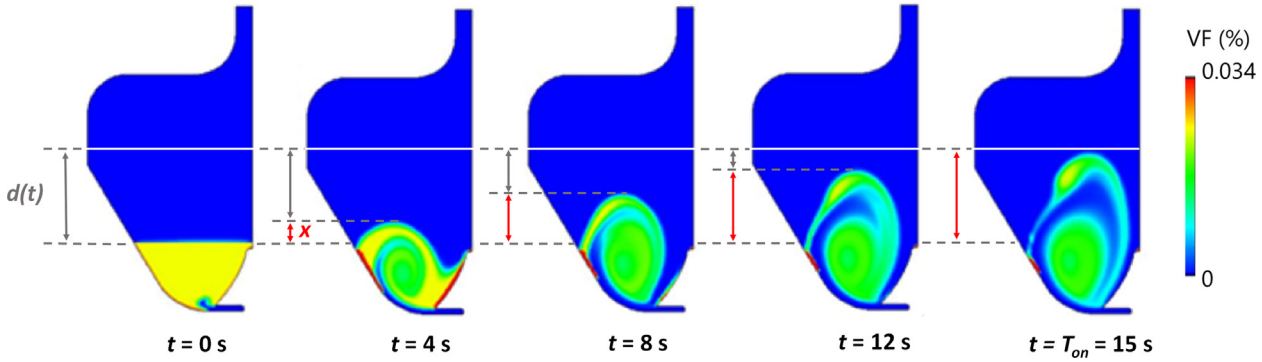

Fig. 4. Computational contour plots of the time evolution of the particle VF within the culture chamber, imposing a T_{on} of 15 s, a particle diameter of 180 μm, a flow rate of 100 mL/min, and an initial particle suspension volume of 10 mL.

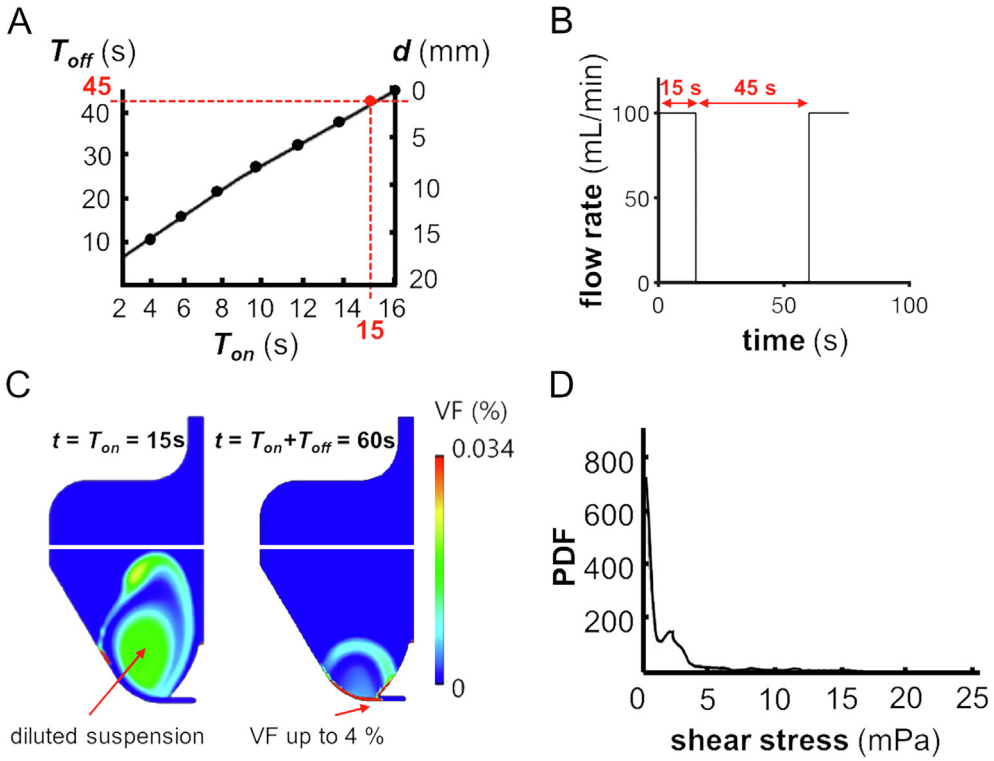

Fig. 5. *In silico* results of the hiPSC explanatory test (particle diameter = 180 μm, flow rate = 100 mL/min, initial particle suspension volume = 10 mL). (A) Operational guideline graph used for setting up the computational pulsed working conditions. (B) Pulsed flow rate waveform resulting from the operational guideline graph, and successively applied as inlet boundary condition for the simulation of three working cycles. (C) Computational contour plots of the VF distribution of the particle cloud within the culture chamber at the end of T_{on}, and at the end of the working cycle. (D) Probability density function (PDF) showing the distribution of the shear stress values experienced by the particle cloud when the pump is on.

(t = 15 s) equal to 1 mm (on the right y axis in Fig. 5A), corresponding to a variation *x(t = 15 s)* equal to 17 mm. Eventually, the value of the time interval T_{off} assuring suspension in the chamber was obtained (45 s, on the left y axis in Fig. 5A). Additional examples of operational graphs, resulting from simulations carried out with settings reported in Table 1, are presented in Supplementary Material.

Once the pulsatile culture conditions were identified using the operational guideline graph (Fig. 5A), the pulsed flow waveform (Fig. 5B) was imposed in the computational model. The simulations, modeling suspended hiPSC aggregates, constituted an *a priori* evaluation of the effectiveness of the identified alternation of flow-driven transport and free-fall motion in assuring unpacked suspension within the culture chamber (Fig. 5C). The simulations confirmed that: (1) at the end of time interval T_{on}, an almost uniform VF distribution (around the prescribed initial value of 2.5×10^{-2}%) was guaranteed; (2) only a marginal packing phenomenon was observed at the end of the working cycle, occupying a very limited region at the bottom of the culture chamber (with VF values up to 4%, but involving approximately only the 0.4% of the cultured particles); (3) suspended particles experienced very low shear stress levels (the observed 90th percentile value of the shear stress distribution within the culture chamber was approximately equal to 10 mPa when the pump was switched on, Fig. 5D); (4) imposing an initial fully anoxic condition within the culture chamber, dissolved oxygen was almost completely replenished after 780 s (Supplementary Material, Movie S1).

3.2. In vitro cell culture verification test

To confirm the effectiveness of the proposed methodology, pre-formed hiPSC aggregates (Fig. 6A) were cultured within the bioreactor adopting the conditions identified using the operational guideline graph (T_{on} = 15 s, T_{off} = 45 s, pulsation period = 60 s at 100 mL/min). After 24 h of pulsed dynamic culture the bioreactor was stopped and no sedimentation was detected. The imposition of the pulsed flow strategy resulted in a final viable-cell density equal to 1×10^6 cell/mL. Light microscopy images display that aggregates cultured under pulsatile flow maintained their spherical morphology (Fig. 6B), with correspondent circularity index equal to 0.74 ± 0.14, comparable with aggregates inoculated at time t_0 (0.76 ± 0.13, Fig. 6C). In terms of size homogeneity, the probability density function (PDF) of the aggregate diameters (Fig. 6D) shows that aggregates cultured under pulsatile condition were characterized by a narrow distribution of their diameters, with few fused aggregates and an average diameter equal to 176 ± 29 μm, comparable with aggregates dimension at inoculation (average diameter = 180 ± 18 μm).

As further indirect confirmation of the proper suspension conditions guaranteed by the pulsed mode, an additional *in vitro* test was performed imposing a continuous flow rate (100 mL/min). This flow regime led to a final viable-cell density of approximately 0.76×10^6 cell/mL. Harvested hiPSC aggregates presented amorphous morphology (Fig. 6B), with circularity index equal to 0.50 ± 0.17 (Fig. 6C), and were characterized by a larger diameter distribution, with diameter values higher than 300 μm (probably due to coalescent aggregates) and an average diameter equal to 183 ± 68 μm (Fig. 6D).

4. Discussion

In recent years, 3D dynamic suspension culture has been demonstrated to be an effective alternative to standard monolayer culture for several applications (Amit et al., 2010; Baghbaderani et al., 2008; Chimenti et al., 2017; Kempf et al., 2014; Rosellini et al., 2018), and different dynamic culture devices have been proposed for this purpose (Gerecht-Nir et al., 2004; Kropp et al., 2017). A crucial contribution towards a comprehensive knowledge of the dynamic culture environment could come from computational modelling, which is becoming a powerful investigation methodology for an efficient tuning of the operational culture parameters, minimizing the number of *in vitro*-setup experiments, thus overcoming time-consuming and expensive trial-and-error approaches for the definition of the optimal bioprocess conditions (Cioffi et al., 2006; Hutmacher and Singh, 2008; Martin et al., 2004; Lyons et al., 2016; Massai et al., 2014). The aim of this work was to propose a robust methodology, based on the combination of computational and analytical approaches, to define *a priori* the hydrodynamic working parameters of a culture device (Massai et al., 2016) used as paradigmatic example of dynamic suspension bioreactor.

A total number of 43 simulations was run to characterize the advective transport within the device depending on imposed flow rate, particle diameter, and initial particle suspension volume (Table 1). In particular, to avoid particle sedimentation and particle adhesion to the filter, non-stationary flow protocols based on pulsed flow rate waveforms were imposed. The pulsed mode allowed generating particle dynamic suspension by (1) advective particle transport, when the pump is on the developing flow structures transport the particles, and (2) free-fall particle motion, when

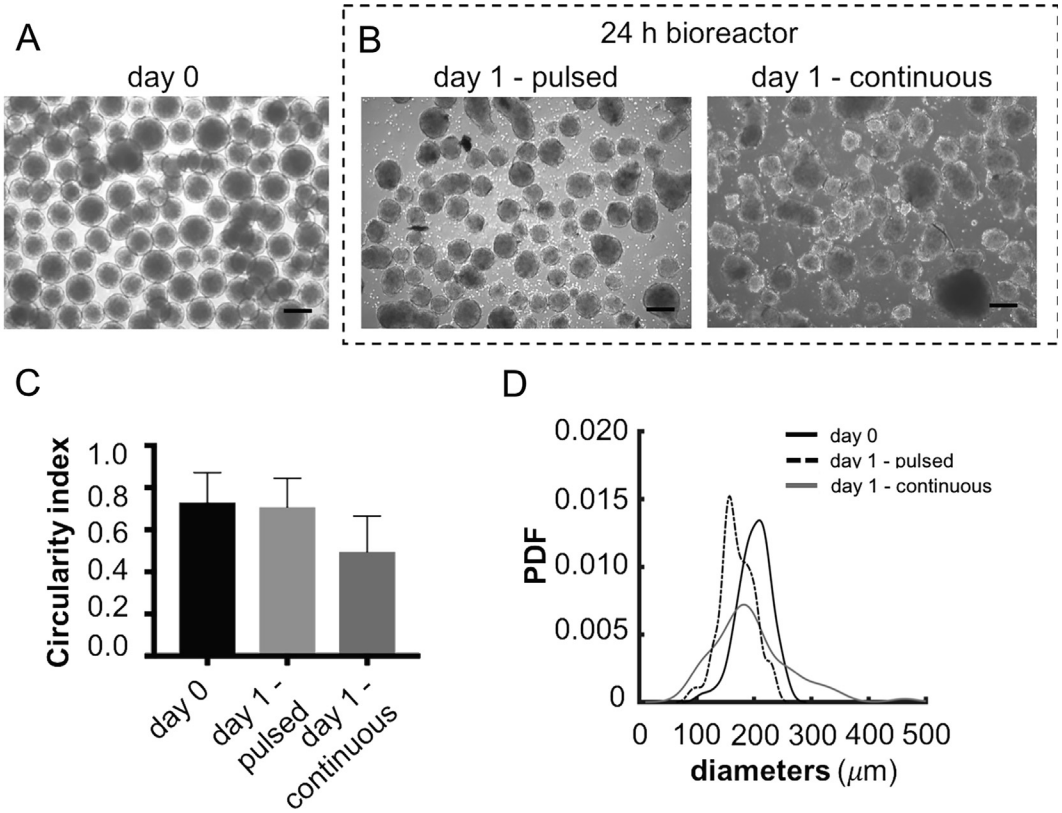

Fig. 6. *In vitro* results of the hiPSC explanatory test. (A) Light microscopy image of pre-formed hiPSC aggregates at day 0, before bioreactor inoculation (scale bar = 200 μm). (B) Light microscopy images of hiPSC aggregates harvested after 24 h of pulsed or continuous flow culture within the bioreactor (scale bar = 200 μm). (C) Circularity index of hiPSC aggregates calculated at day 0, day 1 after 24 h of pulsed flow culture within the bioreactor, and day 1 after 24 h of continuous flow culture within the bioreactor. (D) PDF distributions of the hiPSC aggregate diameters calculated at day 0, day 1 after 24 h of pulsed flow culture within the bioreactor, and day 1 after 24 h of continuous flow culture within the bioreactor.

the pump is off only gravitational force acts upon the particles (Fig. 2).

From *in silico* data and for each simulated time interval T_{on} during which the pump works, the distance $d(t)$ between the particle cloud and the filter and its variation $x(t)$ were calculated. By combining these results with the analytical calculations of the free-fall time interval T_{off}, and imposing highly diluted particle suspensions, 43 different combinations and relative operational guideline graphs were obtained. The computational approach allowed for an *a priori* investigation of the effect of input parameters (i.e., flow rate, flow rate waveform, working cycle duration, particle suspension conditions).

To verify the proposed methodology, we performed an *in vitro* proof-of-principle test culturing hiPSC aggregates for 24 h within the bioreactor. By using the relative operational guideline graph (particle diameter = 180 μm, flow rate = 100 mL/min, initial particle suspension volume = 10 mL, Fig. 5A), the pulsatile working conditions were identified (T_{on} = 15 s, T_{off} = 45 s, pulsation period = 60 s, Fig. 5B), and adopted both for the *in silico* simulation and for the *in vitro* test. Simulations showed that, within the culture chamber, the imposed pulsed flow rate: (1) maintained a uniform and diluted distribution of particles (Fig. 5C); (2) avoided sedimentation regions (Fig. 5C); (3) guaranteed low shear stress levels (Fig. 5D); (4) ensured an efficient, mainly advection-driven transport of dissolved oxygen (Supplementary Material, Movie S1). These results were corroborated by the *in vitro* explanatory test, in which the identified pulsed flow regime avoided hiPSC aggregate sedimentation and, under low-shear stress conditions, preserved hiPSC viability (see Supplementary Material) and aggregate circularity (Fig. 6C), with a narrow distribution of their diameters (Fig. 6D). In the perspective of dynamic culture devices for pluripotent stem cell expansion, the pulsed working conditions identified by the operational graph enabled modulating and controlling hiPSC agglomeration kinetics, avoiding culture heterogeneity that can affect maintenance of pluripotency and interfere with lineage-specific differentiation, thwarting process reproducibility and efficiency (Zweigerdt, 2009; Massai et al., 2017). Conversely, when the bioreactor was run imposing a continuous flow rate (as negative control), agglomeration was promoted and bigger, amorphous and heterogeneous hiPSC aggregates were harvested (Fig. 6C and D).

In this study, the *in silico* model was based on defined assumptions which could influence the simulation outcomes. Firstly, we considered spherical non-deformable particles with constant diameter, both for the *in silico* and analytical calculations. However, in the *in vitro* applications, suspended particles can be characterized by variable diameters and/or irregular shapes (Kumar and Starly, 2015; Wu et al., 2014). In parallel, the inhomogeneity of particle diameters could determine different timing in the free-fall motion, causing a more complex behavior of the particle cloud. Nevertheless, these assumptions were reasonable for hiPSC culture, characterized by regular, rounded shape, and tight diameter distribution. Moreover, the model does not take into account cell proliferation and aggregation, however these are events with time scales of days, while the presented model was designed to describe the early stage of the culture and to provide the working conditions to be set for the explanatory *in vitro* test. Lastly, the duration of the *in vitro* test was 24 h, the minimum time for a first and quick readout of the maintenance of optimal viability, size and morphology of the hiPSC aggregates (Zweigerdt et al., 2011). Longer culture periods would be useful to investigate the effect of the pulsed flow on hiPSC aggregates in terms of proliferation and pluripotency maintenance, but this falls outside of the work aims.

In conclusion, the systematic application of a combined computational-analytical approach allowed for the *a priori* definition of a wide range of hydrodynamic working conditions for the adopted bioreactor. The herein proposed methodology, potentially adaptable to other dynamic suspension devices, could consistently support experimental studies by providing an *in silico*-based *a priori* knowledge useful to limit costs and to ultimately optimize complex dynamic culture bioprocesses.

Declaration of Competing Interest

There are no conflicts of interest.

Acknowledgements

This work was partially supported by the European Union FP7-NMP Programme (BIOSCENT, grant 214539) and by the Italian Ministry of Education, University and Research (NOP for Research and Competitiveness 2007–2013, IRMI (CTN01_00177_888744)). Diana Massai was partially funded by the Horizon 2020 Marie Skłodowska-Curie Individual Fellowship POSEIDON (grant 660480). Robert Zweigerdt was funded by the German Research Foundation (grants ZW64/4-1 and KFO311 ZW64/7-1), by the German Federal Ministry of Education and Research (grants 13N14086, 01EK1601A, 01EK1602A), by StemBANCC (support from the Innovative Medicines Initiative joint undertaking under grant 115439-2, whose resources are composed of financial contribution from the European Union FP7/2007-2013 and EFPIA companies in kind contribution), and by the European Union (TECHNOBEAT, grant 66724).

Appendix A. Supplementary material

Supplementary data to this article can be found online at https://doi.org/10.1016/j.jbiomech.2019.07.021.

References

Abecasis, B., Aguiar, T., Arnault, E., Costa, R., Gomes-Alves, P., Aspegren, A., Serra, M., Alves, P.M., 2017. Expansion of 3D human induced pluripotent stem cell aggregates in bioreactors: bioprocess intensification and scaling-up approaches. J. Biotechnol. 246, 81–93.

Amit, M., Chebath, J., Margulets, V., Laevsky, I., Miropolsky, Y., Shariki, K., Peri, M., Blais, I., Slutsky, G., Revel, M., Itskovitz-Eldor, J., 2010. Suspension culture of undifferentiated human embryonic and induced pluripotent stem cells. Stem Cell Rev. 6 (2), 248–259.

Baghbaderani, B.A., Behie, L.A., Sen, A., Mukhida, K., Hong, M., Mendez, I., 2008. Expansion of human neural precursor cells in large-scale bioreactors for the treatment of neurodegenerative disorders. Biotechnol. Prog. 24 (4), 859–870.

Cherry, R.S., 1993. Animal cells in turbulent fluids: details of the physical stimulus and the biological response. Biotechnol. Adv. 11 (2), 279–299.

Chimenti, I., Massai, D., Morbiducci, U., Beltrami, A.P., Pesce, M., Messina, E., 2017. Stem cell spheroids and ex vivo niche modeling: rationalization and scaling-up. J. Cardiovasc. Translat. Res. 10 (2), 150–166.

Cioffi, M., Boschetti, F., Raimondi, M.T., Dubini, G., 2006. Modeling evaluation of the fluid-dynamic microenvironment in tissue-engineered constructs: a micro-CT based model. Biotechnol. Bioeng. 93 (3), 500–510.

Consolo, F., Bariani, C., Mantalaris, A., Montevecchi, F., Redaelli, A., Morbiducci, U., 2012. Computational modeling for the optimization of a cardiogenic 3D bioprocess of encapsulated embryonic stem cells. Biomech. Model. Mechanobiol. 11 (1–2), 261–277.

Consolo, F., Fiore, G.B., Truscello, S., Caronna, M., Morbiducci, U., Montevecchi, F.M., Redaelli, A., 2009. A computational model for the optimization of transport phenomena in a rotating hollow-fiber bioreactor for artificial liver. Tissue Eng. Part C Methods 15 (1), 41–55.

dos Santos, F.F., Andrade, P.Z., da Silva, C.L., Cabral, J.M., 2013. Bioreactor design for clinical-grade expansion of stem cells. Biotechnol. J. 8 (6), 644–654.

Dusting, J., Sheridan, J., Hourigan, K., 2006. A fluid dynamics approach to bioreactor design for cell and tissue culture. Biotechnol. Bioeng. 94 (6), 1196–1208.

Gerecht-Nir, S., Cohen, S., Itskovitz-Eldor, J., 2004. Bioreactor cultivation enhances the efficiency of human embryoid body (hEB) formation and differentiation. Biotechnol. Bioeng. 86, 493–502.

Godara, P., McFarland, C.D., Nordon, R.E., 2008. Design of bioreactors for mesenchymal stem cell tissue engineering. J. Chem. Technol. Biotechnol. 83, 408–420.

Guilak, F., Butler, D.L., Goldstein, S.A., Baaijens, F.P., 2014. Biomechanics and mechanobiology in functional tissue engineering. J. Biomech. 47 (9), 1933–1940.

Gupta, P., Ismadi, M.Z., Verma, P.J., Fouras, A., Jadhav, S., Bellare, J., Hourigan, K., 2016. Optimization of agitation speed in spinner flask for microcarrier structural integrity and expansion of induced pluripotent stem cells. Cytotechnology 68 (1), 45–59.

Hutmacher, D.W., Singh, H., 2008. Computational fluid dynamics for improved bioreactor design and 3D culture. Trends Biotechnol. 26, 166–172.

Ismadi, M.Z., Gupta, P., Fouras, A., Verma, P., Jadhav, S., Bellare, J., Hourigan, K., 2014. Flow characterization of a spinner flask for induced pluripotent stem cell culture application. PLoS ONE 9 (10), e106493.

Kaiser, S.C., Jossen, V., Schirmaier, C., Eibl, D., Brill, S., van den Bos, C., Eibl, R., 2012. Fluid flow and cell proliferation of mesenchymal adipose-derived stem cells in small-scale, stirred, single use bioreactors. Chem. Ing. Tech. 85, 95–102.

Kempf, H., Olmer, R., Kropp, C., Ruckert, M., Jara-Avaca, M., Robles-Diaz, D., Franke, A., Elliott, D.A., Wojciechowski, D., Fischer, M., Roa, Lara A., Kensah, G., Gruh, I., Haverich, A., Martin, U., Zweigerdt, R., 2014. Controlling expansion and cardiomyogenic differentiation of human pluripotent stem cells in scalable suspension culture. Stem Cell Rep. 3 (6), 1132–1146.

Kinney, M.A., Sargent, C.Y., McDevitt, T.C., 2011. The multiparametric effects of hydrodynamic environments on stem cell culture. Tissue Eng. Part B: Rev. 17, 249–262.

Kropp, C., Massai, D., Zweigerdt, R., 2017. Progress and challenges in large-scale expansion of human pluripotent stem cells. Process Biochem. 59, 244–254.

Kumar, A., Starly, B., 2015. Large scale industrialized cell expansion: producing the critical raw material for biofabrication processes. Biofabrication 7 (4), 044103.

Leung, H.W., Chen, A., Choo, A.B., Reuveny, S., Oh, S.K., 2011. Agitation can induce differentiation of human pluripotent stem cells in microcarrier cultures. Tissue Eng. Part C Methods 17 (2), 165–172.

Lyons, J.S., Iyer, S.R., Lovering, R.M., Ward, C.W., Stains, J.P., 2016. Novel multi-functional fluid flow device for studying cellular mechanotransduction. J. Biomech. 49 (16), 4173–4179.

Martin, I., Wendt, D., Heberer, M., 2004. The role of bioreactors in tissue engineering. Trends Biotechnol. 22 (2), 80–86.

Massai, D., Pennella, F., Gentile, P., Gallo, D., Ciardelli, G., Bignardi, C., Audenino, A., Morbiducci, U., 2014. Image-based three-dimensional analysis to characterize the texture of porous scaffolds. Biomed Res. Int., 161437

Massai, D., Isu, G., Madeddu, D., Cerino, G., Falco, A., Frati, C., Gallo, D., Deriu, M.A., Falvo D'Urso Labate, G., Quaini, F., Audenino, A., Morbiducci, U., 2016. A versatile bioreactor for dynamic suspension cell culture. Application to the culture of cancer cell spheroids. PLoS ONE 11 (5), e0154610.

Massai, D., Bolesani, E., Robles, Diaz D., Kropp, C., Kempf, H., Halloin, C., Martin, U., Braniste, T., Isu, G., Harms, V., Morbiducci, U., Drager, G., Zweigerdt, R., 2017. Sensitivity of human pluripotent stem cells to insulin precipitation induced by peristaltic pump-based medium circulation: considerations on process development. Sci. Rep. 7 (1), 3950.

Olmer, R., Lange, A., Selzer, S., Kasper, C., Haverich, A., Martin, U., Zweigerdt, R., 2012. Suspension culture of human pluripotent stem cells in controlled, stirred bioreactors. Tissue Eng. Part C Methods 18 (10), 772–784.

Pennella, F., Rossi, M., Ripandelli, S., Rasponi, M., Mastrangelo, F., Deriu, M.A., Ridolfi, L., Kähler, C.J., Morbiducci, U., 2012. Numerical and experimental characterization of a novel modular passive micromixer. Biomed. Microdev. 14 (5), 849–862.

Rodrigues, C.A., Fernandes, T.G., Diogo, M.M., da Silva, C.L., Cabral, J.M., 2011. Stem cell cultivation in bioreactors. Biotechnol. Adv. 29 (6), 815–829.

Rosellini, E., Barbani, N., Frati, C., Madeddu, D., Massai, D., Morbiducci, U., Lazzeri, L., Falco, A., Lagrasta, C., Audenino, A., Cascone, M.G., Quaini, F., 2018. Influence of injectable microparticle size on cardiac progenitor cell response. J. Appl. Biomater. Funct. Mater. 16, 241–251.

Schroeder, M., Niebruegge, S., Werner, A., Willbold, E., Burg, M., Ruediger, M., Field, L.J., Lehmann, J., Zweigerdt, R., 2005. Differentiation and lineage selection of mouse embryonic stem cells in a stirred bench scale bioreactor with automated process control. Biotechnol. Bioeng. 92, 920–933.

Singh, H., Teoh, S.H., Low, H.T., Hutmacher, D.W., 2005. Flow modelling within a scaffold under the influence of uni-axial and bi-axial bioreactor rotation. J. Biotechnol. 19 (2), 181–196.

Sucosky, P., Osorio, D.F., Brown, J.B., Neitzel, G.P., 2004. Fluid mechanics of a spinner-flask bioreactor. Biotechnol. Bioeng. 85 (1), 34–46.

Thouas, G.A., Sheridan, J., Hourigan, K., 2007. A bioreactor model of mouse tumour progression. J. Biomed. Biotechnol., 32754

Warnock, J.N., Al-Rubeai, M., 2006. Bioreactor systems for the production of biopharmaceuticals from animal cells. Biotechnol. Appl. Biochem. 45, 1–12.

Williams, A., Nasim, S., Salinas, M., Moshkforoush, A., Tsoukias, N., Ramaswamy, S., 2017. A "sweet-spot" for fluid-induced oscillations in the conditioning of stem cell-based engineered heart valve tissues. J. Biomech. 65, 40–48.

Wu, J., Rostami, M.R., Olaya, D.P.C., Tzanakakis, E.S., 2014. Oxygen transport and stem cell aggregation in stirred-suspension bioreactor cultures. PLoS ONE 9 (7), e102486.

Zhao, F., van Rietbergen, B., Ito, K., Hofmann, S., 2018. Flow rates in perfusion bioreactors to maximise mineralisation in bone tissue engineering in vitro. J. Biomech. 79, 232–237.

Zweigerdt, R., 2009. Large scale production of stem cells and their derivatives. Adv. Biochem. Eng. Biotechnol. 114, 201–235.

Zweigerdt, R., Olmer, R., Singh, H., Haverich, A., Martin, U., 2011. Scalable expansion of human pluripotent stem cells in suspension culture. Nat. Protoc. 6 (5), 689–700.